

Ferromagnetic $\text{Ga}_{1-x}\text{Mn}_x\text{N}$ epilayers versus antiferromagnetic GaMn_3N clusters

R. Giraud, S. Kuroda*, S. Marcet, E. Bellet-Amalric, X. Biquard, B. Barbara¹, D. Fruchart², D. Ferrand, J. Cibert and H. Mariette

CEA-CNRS group ‘Nanophysique et Semi-conducteurs’, Laboratoire de Spectrométrie Physique, Université Joseph Fourier, and DRFMC-SP2M, CEA Grenoble, 38054 Grenoble, France

¹ *Laboratoire de Magnétisme Louis Néel, CNRS, BP166, 38042 Grenoble, France*

² *Laboratoire de Cristallographie, CNRS, 38042 Grenoble Cedex-09, France*

* *On leave from Institute of Materials Science, Univ. of Tsukuba, Japan*

(May 22, 2019)

Abstract

We report the growth of Mn-doped wurtzite GaN epilayers by nitrogen plasma-assisted molecular beam epitaxy. The incorporation of manganese, achieved up to 18%, is found to be very sensitive to the growth conditions. Below about 2% of Mn, correlated structural and magnetic measurements of GaN:Mn clearly demonstrate that the coexistence of room-temperature ferromagnetism with paramagnetism is an intrinsic property of the pure diluted magnetic semiconductor $\text{Ga}_{1-x}\text{Mn}_x\text{N}$. In particular, high-temperature hysteresis loops reveal inhomogeneous ferromagnetism, which cannot be attributed to superparamagnetism of unresolved magnetic precipitates. At higher Mn contents, GaMn_3N precipitates are evidenced by x-ray diffraction and absorption, and their increasing contribution is no more negligible. These lead, first to a slow magnetic relaxation below 10 K, related to the blocking of small clusters with a finite magnetic moment, and then to a limited magnetisation due to large antiferromagnetic clusters.

Since the discovery of giant magneto-resistance in ferromagnetic metal multilayers [1], spin-dependent phenomena rapidly appeared as a unique mean to merge information storage and processing, thus rising one of the powerful concepts of a spin-based electronics [2]. Nevertheless, metal-semiconductor interfaces could hinder the injection of a spin-polarized current into a semiconductor [3], although an additional tunneling barrier is predicted to overcome this issue [4,5]. Diluted magnetic semiconductors (DMS -see, e.g., [6,7]-) showing room-temperature ferromagnetism appear as a serious alternative to ferromagnetic metals to ensure an efficient injection and, indeed, high critical temperatures T_c were predicted in Mn-doped wide band-gap semiconductors [8]. As a result, there is a growing interest in the search for DMS having both a high T_c value and a large spin polarization of the carriers, which could then be used as spin polarizers or filters and for spin injection into a nonmagnetic semiconductor (similarly to other DMS which were used at low temperatures [9,10]). Room-temperature ferromagnetism was previously reported in GaN:Mn thick films [11–13], with an extrapolated $T_c \sim 940$ K [11]. However, these results remain ambiguous: a large additional paramagnetic component is also observed [14–16], and ferrimagnetic clusters, such as Mn₄N precipitates with the perovskite structure, could be at the origin of a ferromagnetic-like behaviour [17–19].

In order to determine the specific features of the pure Ga_{1-x}Mn_xN phase, we investigated in detail the structural and magnetic properties of GaN:Mn thick epilayers with the wurtzite structure. These were grown by nitrogen-plasma assisted molecular beam epitaxy (MBE) on a GaN buffer layer, previously elaborated by metal-organic chemical vapor deposition on a sapphire substrate. The manganese content was always checked by secondary ion mass spectrometry (SIMS), using an Mn-implanted GaN layer as a reference: depth profiles were homogeneous over the 0.3 micron layer thickness. As discussed below, no evidence of any secondary phase was found for Mn incorporations as large as 2%, using extended x-ray absorption spectroscopy (EXAFS) as a local probe of the Mn environment, whereas we give direct evidences for the formation and the nature of antiferromagnetic precipitates with the perovskite structure above 2%. At low Mn contents, high-temperature hysteresis loops ($T \leq 400$ K in our experiment) cannot be explained in term of superparamagnetism of unresolved magnetic clusters with a distribution of blocking temperatures, both from the amplitude and the temperature-dependence points of view. Moreover, an additional paramagnetic component is also evidenced at low temperature. This coexistence of magnetic phases, as well as a detailed analysis of the ferromagnetic component, strongly suggest that inhomogeneous properties occur in our diluted Ga_{1-x}Mn_xN epilayers, which are not due to clusters of another phase.

The MBE-growth of GaN was previously studied in detail [20,21]. It was shown that the growth front of GaN strongly depends on the Ga/N flux ratio. Under N-rich conditions, a rough N-terminated surface is formed, which is stable when growth is stopped. Under Ga-rich conditions, a wetting Ga film is formed, which can be evidenced by the dwell time of the reflection high-energy electron diffraction (RHEED) transient signal during the growth interruption: a thorough calibration shows that this dwell time is a measure of the Ga-film desorption [21]. At low Ga excess, the Ga surface coverage increases with the Ga flux. At intermediate Ga flux, a plateau is observed (fig. 1a), which corresponds to the formation of a self-regulated bilayer of Ga at the growth front. This smooth surface stabilizes a 2D growth of GaN within a finite growth window so that, the growth is fairly insensitive to fluctuations

of the Ga flux and of the substrate temperature. The addition of a Mn flux reduces both the width of this plateau (fig. 1a), and the growth rate under N-rich conditions (fig. 1b): both effects point to a reduction of the Ga sticking coefficient, which tends to limit the self-regulated 2D growth of Mn-doped GaN epilayers. Finally, at even larger Ga flux, Ga droplets are formed, as evidenced by the increase of the Ga desorption time (fig. 1a). Therefore, it is important to have a precise knowledge of this diagram (fig. 1a), since the Mn incorporation, for a given Mn flux, strongly depends on the growth regime [22]. A significant amount of manganese, up to 18%, was incorporated under N-rich conditions, close to stoichiometry, whereas the incorporation of Mn was reduced under Ga-rich conditions within the self-regulated growth window: for a low-enough given Mn flux, the Mn content is found to be ten times smaller under Ga-rich conditions as compared to the N-rich case. This behaviour may be attributed to a decrease of the Mn sticking coefficient when the Ga surface coverage is increased or may suggest that the Ga bilayer acts as a diffusion barrier hindering the incorporation into GaN.

The epilayers structure was studied using a SEIFERD 3003 PTS-HR x-ray diffractometer. The measurements do not show any spurious phase for a Mn content smaller than 2%, whereas the formation of additional clusters with the perovskite structure is evidenced at larger doping levels (fig. 2). These could be either GaMn_3N or Mn_4N clusters: as these two phases have nearly the same lattice parameter [23], one cannot distinguish between them by x-ray diffraction. These precipitates show two crystalline orientations, and most have their [111] direction (three-fold axis) colinear to the wurtzite *c*-axis. Note that, using a vicinal silicon surface ($\sim 4^\circ$ off) as a sample holder to achieve a low background, the large dynamical range allows us to evidence the presence of these oriented clusters for a Mn-content down to about 2% of Mn, instead of 6% in [19]. Although a small amount of tiny clusters cannot be excluded (less than a few percents, because of the measurement accuracy given by our small but finite background), the higher sensitivity of x-ray absorption measurements also allows us to demonstrate the absence of such precipitates below about 2% of Mn.

We performed EXAFS measurements at the Mn K-edge on both our GaN:Mn epilayers and two perovskite powders, at the European Synchrotron Radiation Facility. This analysis was intended, first to completely discard the occurrence of any other phase but the purely diluted $\text{Ga}_{1-x}\text{Mn}_x\text{N}$ one at low-enough Mn contents and, second, to clearly identify the precipitates present at larger Mn incorporations. Indeed, the local environment is much different for a Mn either in GaMn_3N or Mn_4N clusters, both with the perovskite structure, and for a Mn substituting a Ga in wurtzite GaN: there are 2N as nearest-neighbours in the perovskite instead of 4N in the wurtzite, and the bond lengths are shorter. Moreover, the second neighbours allow one to distinguish GaMn_3N (8Mn+4Ga) from Mn_4N (12Mn). Two contrasted behaviours in EXAFS oscillations are observed in fig. 3a, at low or high Mn contents, whereas intermediate Mn contents above 2% exhibit a gradual change from one case to the other (not shown). The Fourier transforms of these weighted oscillations (fig. 3b) give distances to the central Mn ion that are in agreement with either the wurtzite or the perovskite structures, respectively.

For a 1.5% Mn-doped GaN epilayer, the measurement can be fitted to a calculation based on a Mn random substitution of Ga in wurtzite GaN, including the first seven shells, which shows that the pure $\text{Ga}_{1-x}\text{Mn}_x\text{N}$ phase is obtained (with $x = 1.5\%$). The two additional peaks evidenced at large *R* values in fig. 3b can also be reproduced if the first thirteen

shells are taken into account in the calculation, but without considering multiple scattering paths. However, these neglected paths contribute to the exact shape of the peaks, so that we only considered the first seven shells for the accurate fit shown in fig. 3b. On the contrary, for a 18% Mn-doped GaN epilayer, EXAFS oscillations are strongly modified and now clearly fit the experimental oscillations of a GaMn_3N powder (note that these oscillations are perfectly in phase, up to large k values). This demonstrates that most of the manganese ions contribute to this perovskite phase in the high-doping range. Moreover, it is clear from the experimental data (shift and amplitude, see fig. 3a -up-) that the EXAFS oscillations of this 18% Mn-doped GaN epilayer do not fit the ones obtained with a Mn_4N powder. This result is also corroborated by x-ray absorption near edge structure (XANES) measurements, showing identical edges for both our highest Mn-doped GaN epilayer and the GaMn_3N powder, whereas a shift of about 2 eV is revealed for the Mn_4N one (not shown). All these features allow us to clearly identify the perovskite precipitates as due to GaMn_3N clusters and not to Mn_4N ones. This is particularly important since GaMn_3N is antiferromagnetic while Mn_4N is ferrimagnetic [23,24].

Magnetisation measurements were performed using a MPMS-Quantum Design SQUID magnetometer, with an improved accuracy achieved with a reciprocating sample technique, the magnetic field being applied within the layer plane, that we checked to be the easy plane. We paid much attention to accurately subtract the large diamagnetic contribution of the substrate. This is particularly difficult at low temperatures for the small paramagnetic signals measured. Therefore, we mainly ruled out any significant non linear contribution from the substrate and used the fully saturated magnetisation, as observed in high fields below $T \sim 5$ K, to subtract the diamagnetic component. As above, we concentrate on the two extreme cases involving either a low Mn content, for which only the purely diluted $\text{Ga}_{1-x}\text{Mn}_x\text{N}$ phase is obtained, or the highest Mn incorporation showing a large amount of GaMn_3N precipitates.

Fig. 4 shows the magnetic behaviour of a $\text{Ga}_{1-x}\text{Mn}_x\text{N}$ epilayer grown under Ga-rich conditions with $x \sim 0.3\%$, that is, being far away from the smaller concentration at which additional precipitates were evidenced. Hysteresis loops are observed up to 400 K (the highest temperature of our experimental setup) with a temperature-independent slope around zero-field, which strongly suggests the occurrence of room-temperature ferromagnetism in the diluted magnetic semiconductor $\text{Ga}_{1-x}\text{Mn}_x\text{N}$ (fig. 4a). Moreover, the small remanent magnetisation is slowly decreasing with increasing temperature and remains finite up to 400 K, showing that the collective behaviour in this epilayer is characterised by $T_c > 400$ K. However, the high-temperature saturated magnetisation of about 0.7 emu/cm³ is rather weak and it amounts only to $0.9 \mu_B/\text{Mn}$ (fig. 4a, inset), the total amount of Mn atoms being accurately measured by SIMS. Actually, a temperature-dependent paramagnetic contribution, being clearly observed at low temperatures and in high fields, is superimposed on the ferromagnetic one (fig. 4b). The saturated magnetisation at 4 K, of about 5 emu/cm³, gives the right order of magnitude for a Mn localized magnetic moment, that is close to $5 \mu_B$, but does not allow to conclude quantitatively about the valence state. From a comparison of the saturated magnetisation at 4 K and 400 K, only about 15% of the Mn ions contribute to ferromagnetism. Moreover, the temperature-independent low-field susceptibility at high temperature is much smaller than the one expected from shape anisotropy. This might make more difficult the ferromagnetic contribution to be observed at low temperatures, compared

to the larger paramagnetic component, especially if a field perpendicular to the plane is applied [16]. As we did not find any significant anisotropy within the film plane, this small initial slope could suggest inhomogeneous ferromagnetic properties. A similar behaviour was observed at other Mn contents. In particular, ferromagnetism is also revealed in the sample shown in fig. 3, with $x \sim 1.5\%$.

Contrary to the low Mn content case, the magnetic moment per Mn is found to be strongly reduced in a GaN:Mn epilayer containing a much larger amount of manganese ions ($\sim 18\%$): only about $0.1 \mu_B/\text{Mn}$ at 400 K (fig. 4a inset) and less than $0.5 \mu_B/\text{Mn}$ at low temperature. This magnetic behaviour shows that most of the manganese ions ($\sim 90\%$) now incorporate into the GaMn_3N precipitates, thus corroborating EXAFS measurements, and demonstrates that these clusters are large enough to have a bulk-like antiferromagnetic behaviour [23]. More complicated results are expected at intermediate manganese compositions, when GaMn_3N precipitates are small enough to also contribute to the whole magnetisation, due to deviations from long-range antiferromagnetic ordering. This could lead to an optimum in the magnetisation [13], with some hysteresis related to the coexistence of both ferromagnetic $\text{Ga}_{1-x}\text{Mn}_x\text{N}$ and very small GaMn_3N precipitates with a finite magnetisation. Furthermore, a slow magnetic relaxation component was also evidenced below 10 K in a 1.7% Mn-doped GaN epilayer and at higher intermediate Mn contents. Nevertheless, this contribution remains rather small compared to the ferromagnetic component, and may be due to either an inhomogeneous distribution of Mn ions [27] or, more probably, the freezing of small superparamagnetic clusters.

To sum up, this study shows that diluted $\text{Ga}_{1-x}\text{Mn}_x\text{N}$ epilayers which do not contain any secondary phase, exhibit an intrinsic inhomogeneous ferromagnetic behaviour at room temperature. However, only a small fraction of the manganese impurities ($\sim 15\%$ for $x \sim 0.3\%$) is involved in the collective magnetic phase, while others remain in a paramagnetic state. Nevertheless, the associated magnetic hysteresis cannot be attributed to unresolved magnetic precipitates, mainly because large blocking temperatures are ruled out in tiny clusters with a small anisotropy, and also because EXAFS accuracy is much better than 15%. Moreover, large manganese nitride clusters are either antiferromagnets or highly compensated ferrimagnets. Interestingly, because of this reduced magnetisation, a complete incorporation of Mn ions into large Mn_4N precipitates would only give about $1 \mu_B/\text{Mn}$, that is, less than observed. Other ferrimagnetic compounds, such as MnGa , lead to similar conclusions. Furthermore, the early formation of small GaMn_3N precipitates, which cannot be resolved by x-ray analysis, is evidenced by a slow magnetic relaxation component below 10 K and is absent for $x \leq 1.7\%$ (in this case, less than $\sim 0.1\%$ of Mn ions incorporate into GaMn_3N clusters). In $\text{Ga}_{1-x}\text{Mn}_x\text{As}$, the coexistence of magnetic phases is usually attributed to a random distribution of localized Mn-impurities exchange-coupled to each other by a spatially-inhomogeneous carrier density, which can be expected in a system close to its Mott transition. Yet, an inhomogeneous distribution of Mn ions cannot be excluded. Note, however, that three features make large band-gap ferromagnetic semiconductors quite different from previously studied materials, that is: i) the $3d$ -band as well as the Fermi energy are expected to lie within the gap [28,29], and not within the valence band; ii) conductivity of GaN:Mn layers is often found to be of n -type, instead of p -type as usually required; iii) both the carrier density and the Mn content remain rather small compared to what is required in the p -type carrier-induced model [8]. This suggests that a more complex mechanism could

be at the origin of exchange couplings, and a better understanding of the carrier and Mn ion spatial distributions is necessary to highlight the origin of ferromagnetism in wide band-gap diluted magnetic semiconductors.

Acknowledgements

We thank Y. Genuist for his technical assistance, P. Hollinger, O. Kaitasov and the PROBION company for the SIMS measurements, and O. Proux and J.-L. Hazemann for their support at the ESRF. SK thanks the Japanese Overseas Research Fellow sponsored by Monbukagakush. This work was supported by the EC FENIKS project G5RD-CT-2001-00535.

REFERENCES

- [1] Baibich M. N. *et al.*, Phys. Rev. Lett. **61**, 2472 (1988).
- [2] Wolf S. A. *et al.*, Science **294**, 1488 (2001).
- [3] Schmidt G. *et al.*, Phys. Rev. B **62**, R4790 (2000).
- [4] Rashba E., Phys. Rev. B **62**, R16267 (2000).
- [5] Fert A. & Jaffr  s H., Phys. Rev. B **64**, 184420 (2001).
- [6] Ohno H., Science **281**, 951 (1998).
- [7] Ferrand D. *et al.*, Phys. Rev. B **63**, 085201 (2001).
- [8] Dietl T. *et al.*, Science **287**, 1019 (2000).
- [9] Fiederling R. *et al.*, Nature **402**, 787 (1999).
- [10] Ohno Y. *et al.*, Nature **402**, 790 (1999).
- [11] Sonoda S. *et al.*, J. Cryst. Growth **237-239**, 1358 (2002).
- [12] Reed M. L. *et al.*, Appl. Phys. Lett. **79**, 3473 (2001).
- [13] Thaler G. T. *et al.*, Appl. Phys. Lett. **80**, 3964 (2002).
- [14] Zajac M. *et al.*, Appl. Phys. Lett. **78**, 1276 (2001).
- [15] Soo Y. L. *et al.*, Appl. Phys. Lett. **79**, 3926 (2001).
- [16] Ando K., Appl. Phys. Lett. **82**, 100 (2003).
- [17] Cui Y. & Li L., Appl. Phys. Lett. **80**, 4139 (2002).
- [18] Rao B. K. & Jena P., Phys. Rev. Lett. **89**, 185504 (2002).
- [19] Kim K. H. *et al.*, Appl. Phys. Lett. **82**, 1775 (2003).
- [20] Heying B. *et al.*, J. Appl. Phys. **88**, 1855 (2000).
- [21] Adelmann C. *et al.*, J. Appl. Phys. **91**, 9638 (2002).
- [22] Kuroda S. *et al.*, to be published in Phys. Stat. Solidi.
- [23] Bouchaud J. P., Ann. Chim. **3**, 81 (1968).
- [24] Fruchart D. & Bertaut E. F., J. Phys. Soc. Jpn. **44**, 781 (1978).
- [25] Sato M. *et al.*, Jpn. J. Appl. Phys. **41**, 4513 (2002).
- [26] Biquard X. *et al.*, J. Superconductivity **16**, 792 (2003).
- [27] Dhar S. *et al.*, Appl. Phys. Lett. **82**, 2077 (2003).
- [28] Kulatov E. *et al.*, Phys. Rev. B **66**, 045203 (2002).
- [29] Kronik L., Jain M. & Chelikowsky J. R., Phys. Rev. B **66**, 041203(R) (2002).

LIST OF FIGURES CAPTIONS

FIG. 1 Growth of Mn-doped GaN epilayers. (a), Ga flux dependence of the Ga desorption time, after the growth of GaN (filled squares) and Mn-doped GaN for two values (open triangles and circles) of the Mn-beam equivalent pressure (BEP), the N_2 flow and the substrate temperature being kept constant (surface stoichiometry is achieved close to 0.27 ML/s). (b), Specular RHEED intensity obtained during the growth of both GaN and $Ga_{1-x}Mn_xN$ (with $x \sim 1.7\%$), under N-rich conditions with a Ga flux of 0.23 ML/s. The indicated growth rate is deduced from the RHEED oscillations.

FIG. 2 (a), X-ray θ - 2θ diffraction patterns of GaN:Mn epilayers. For a 18% Mn-doped GaN epilayer, the presence of oriented clusters with the perovskite structure is revealed. An additional AlN buffer layer was also grown for transport measurements. (b), Observation of perovskite clusters at Mn contents larger than about 2%, which are shown to be $GaMn_3N$ precipitates by x-ray absorption.

FIG. 3 Mn local environment in GaN:Mn epilayers. (a), EXAFS oscillations as measured in the two extreme cases, that is, for a Mn content either below 2% or as large as 18%. The latter case is compared with EXAFS oscillations obtained in $GaMn_3N$ and Mn_4N powders, with the perovskite structure. (b), Fourier transforms of the weighted EXAFS oscillations shown in (a), within the k -range $[4.25, 11.7] \text{ \AA}^{-1}$. Using the FEFITT routine package, the calculation based on wurtzite GaN, with a central Ga atom substituted by a Mn atom, takes every interferences paths into account. Including the first seven shells, an accurate fit is obtained, without any additional contribution but a slight change of about 2% in the Mn-N bound length to the first 4N neighbours (see also [15,25,26]).

FIG. 4 Magnetic behaviour in $Ga_{1-x}Mn_xN$ with $x \sim 0.3\%$. (a), Temperature-independent hysteresis loops are observed at temperatures as high as 400 K (the limit of our experimental setup). Inset: the reduced magnetic moment per manganese is even much smaller for the 18% case, due to antiferromagnetic $GaMn_3N$ precipitates. (b), A temperature-dependent paramagnetic component is also revealed at low temperatures, the high-field saturation thus giving a magnetic moment close to $5 \mu_B$.

FIGURES

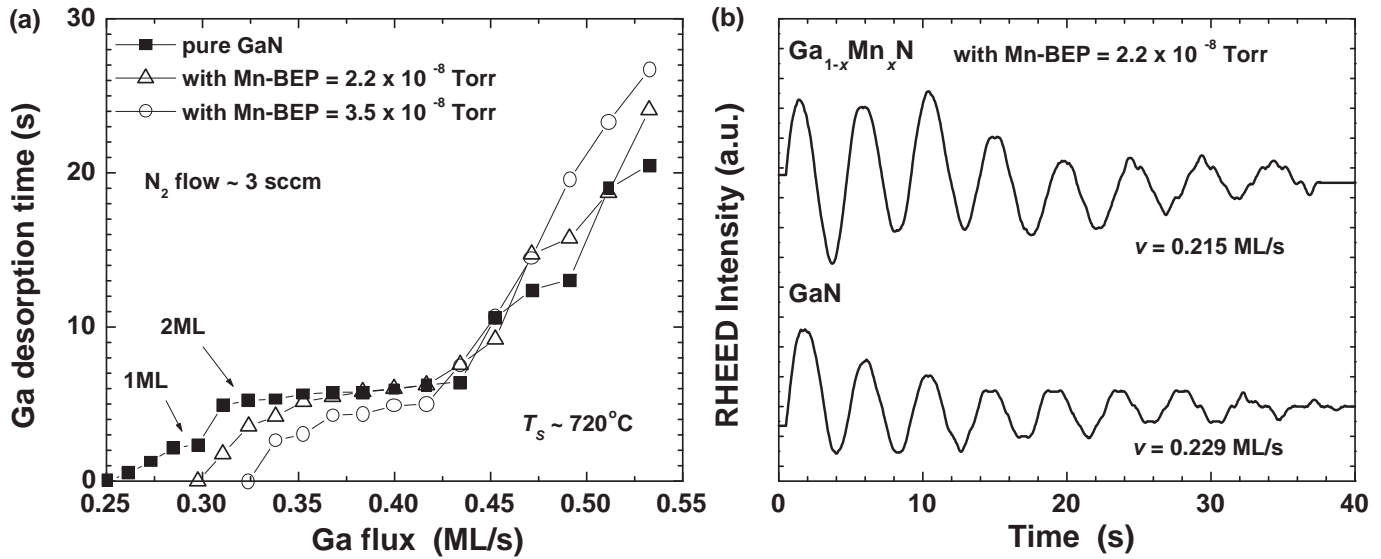


FIG. 1. R. Giraud *et al.*

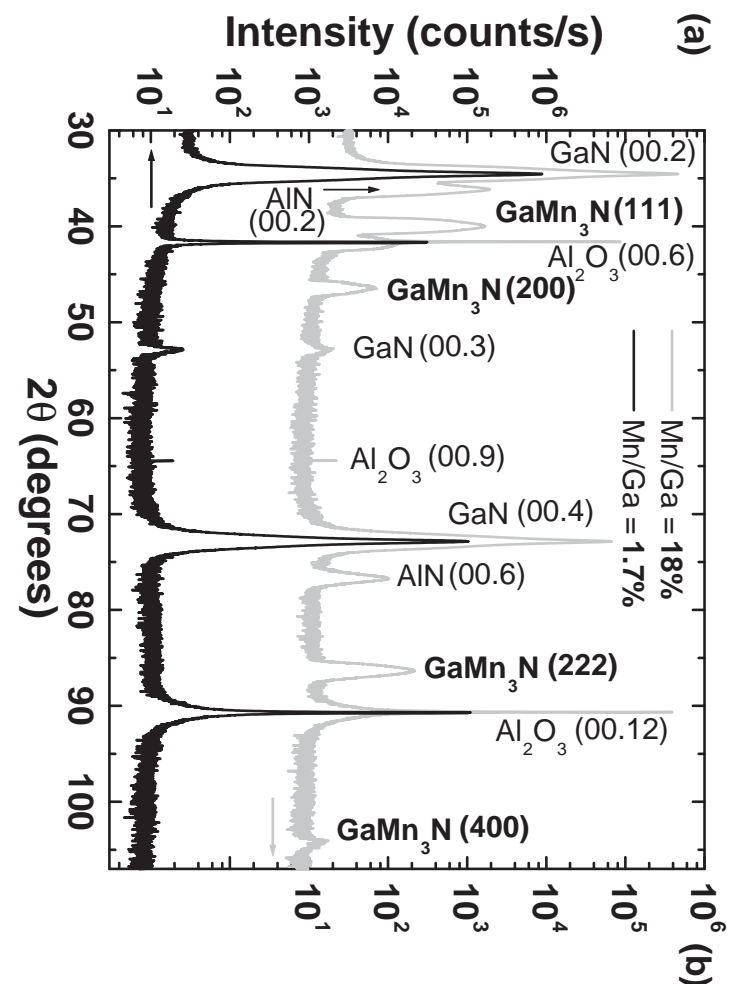
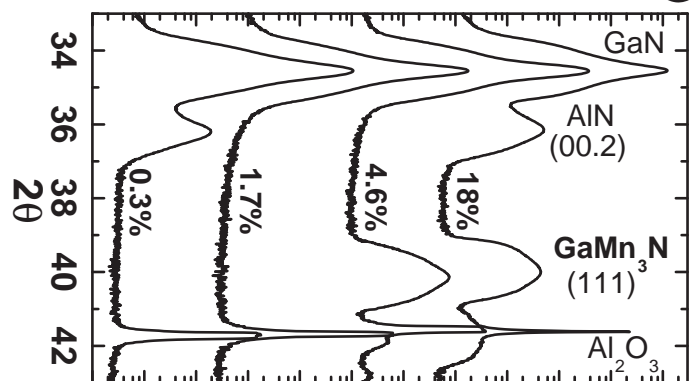


FIG. 2. R. Giraud *et al.*



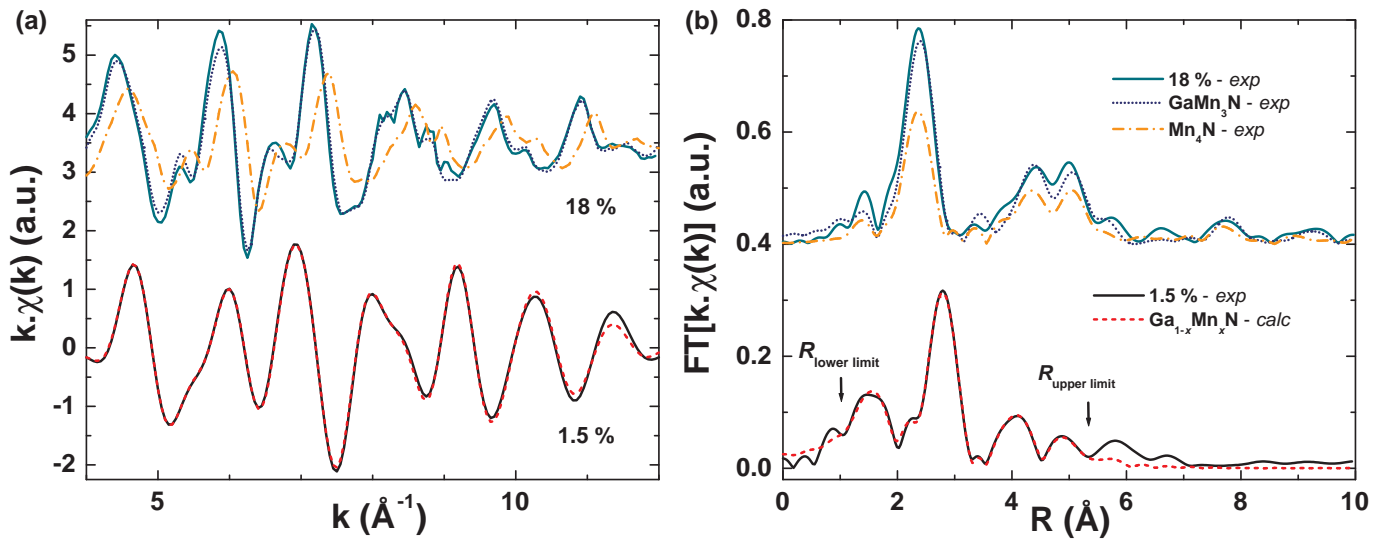


FIG. 3. R. Giraud *et al.*

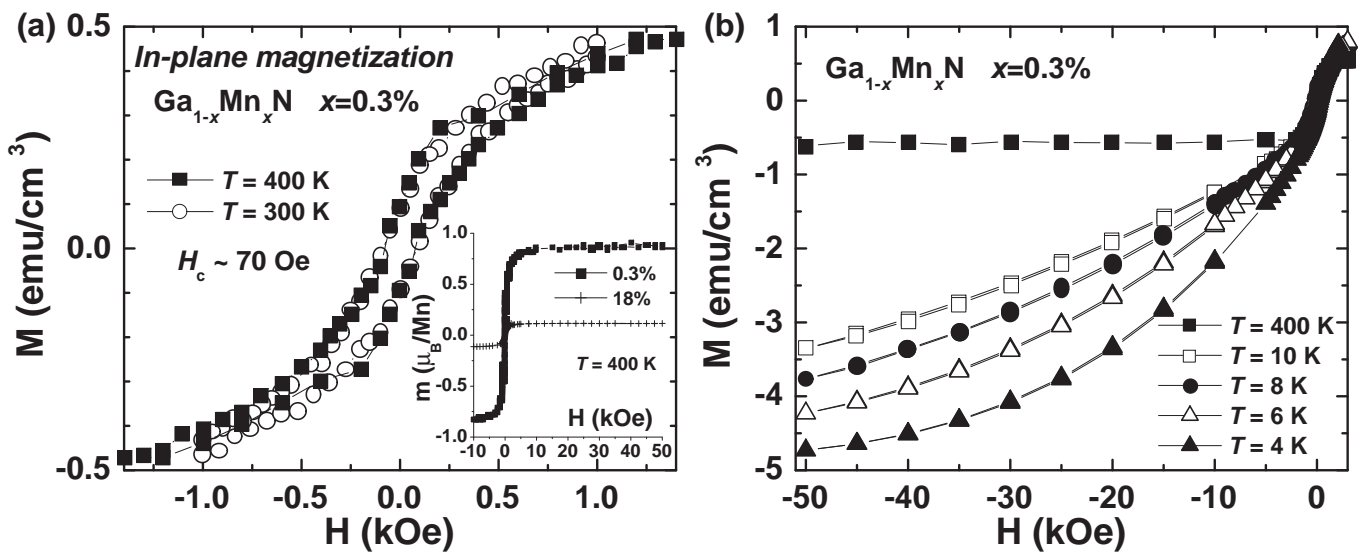


FIG. 4. R. Giraud *et al.*